Air Distribution in Rooms, (ROOMVENT 2000)
Editor: H.B. Awbi

A NUMERICAL INVESTIGATION OF AIRFLOW IN DESIGNATED REFUGE FLOOR

W Z Lu[1], S M Lo[1], Z Fang[2], K K Yuen[1]

[1] Department of Building & Construction, City University of Hong Kong, Kowloon, HK
[2] Department of Architecture and Civil Engineering, Wuhan University of Hydraulic and Electric Engineering, Wuhan, 430072, P R China

Abstract

Refuge floor is specially designed in high-rise building for the purpose of supplying a temporarily safe place for evacuees under emergency situation and is a prescriptive requirement in the fire code of Hong Kong. Such a provision appears to be desirable by the regulators as it relates to simple rules and has administrative convenience. The safety of refuge floor under fire situation may be impaired if the floor is affected by smoke from other levels. The code prescribes that cross-ventilation should be provided in refuge floor so as to prevent smoke logging. However, the adequacy of such measure and the influence of such open floor on the rest of building have not been analytically studied. In this paper, a Computational Fluid Dynamics (CFD) method is employed to analyze the airflow field around and inside a refuge floor. The aim of this paper is to describe the airflow field in and around a designated refuge floor, which is the first step to explore the wind effect on the safety of refuge floors. The study shows that airflow could be a factor affecting the smoke flow pattern.

Keywords: Refuge Floor, Numerical simulation, Cross-ventilation, High-rise building, Airflow pattern, Open-floor, Obstructed-floor, Floor planning

I. Introduction

The space available for erecting buildings in Hong Kong and many other metropolitan cities in Asia is limited. Growth of population, changes in family structure and expansion in business activities cause the demand for built space increasing rapidly in the past two decades. Numerous high-rise or ultra high-rise buildings have been erected in the recent decades and those are normally over 40 storeys. This implies that a large number of people in the Asian region live and work at high levels. There is no doubt that the government authority, the building designers as well as the people of these cities are concerned for the design of high-rise buildings especially for the provisions related to the safety of the occupants inside these buildings. In relation to the emergency escape from high-rise buildings, the Hong Kong Government has stipulated that designated refuge floors should be provided in these buildings [HK Govn., 1996]. Such refuge floor acts as a safe place for a short rest before people continue further escape actions [Egan, 1986, Lo, 1998]. It also acts as a safe passage for people using one staircase once encountering smoke, fire or obstruction there, and enables them to

proceed to an alternative one. Additionally, it acts as an assembly place for people to wait for rescue in case none of staircases can be used due to smoke, fire or obstruction. The code also prescribes that cross-ventilation should be provided in refuge floor so as to prevent smoke logging and guarantee the safety of refuge floors. However, the safety of refuge floor under fire situations may be impaired if it is affected by smoke dispersed from other levels. The smoke dispersion, under fire situation, may be affected by the position of fire source, the presence of wind, and the configuration of buildings, etc. The knowledge on these aspects may have particular importance to the building designers. However, the studies in these areas are very limited. In this paper, a Computational Fluid Dynamics (CFD) technique is applied to analyze wind effect on a high-rise building with designated refuge floor and airflow field inside a refuge floor. It is expected to provide preliminary information about how the existence of designated refuge floor in high-rise building influences the wind loading on building surfaces, the airflow pattern around building and inside the refuge floor. The numerical results will be validated by the available scaled-model test in wind tunnel [Sathopolous, et al, 1989].

II. Mathematical Model and Physical Description

A CFD simulation is carried out to predict the air movement around and inside refuge floor and wind loading on the building surfaces. The geometrical configuration of the model is shown in figure 1. The airflow studied is considered as three-dimensional, steady, isothermal, incompressible and turbulent flow. The governing equations to describe air movement are expressed as:

$$\frac{\partial U_i}{\partial x_i} = 0 \qquad (1)$$

$$U_j \frac{dU_i}{dx_j} = -\frac{1}{\rho}\frac{\partial P}{\partial x_i} + \frac{\partial}{\partial x_j}\left[\nu\left(\frac{\partial U_i}{\partial x_j} + \frac{\partial U_j}{\partial x_i}\right) - \overline{u_i' u_j'}\right] \qquad (2)$$

$$\overline{u_i' u_j'} = -\nu_t\left(\frac{\partial U_i}{\partial x_j} + \frac{\partial U_j}{\partial x_i}\right) + \frac{2}{3}k\delta_{ij} \qquad (3)$$

$$\nu_t = C_\mu \frac{k^2}{\varepsilon} \qquad (4)$$

$$U_j \frac{\partial k}{\partial x_j} = \frac{\partial}{\partial x_j}\left[\left(\nu + \frac{\nu_t}{\sigma_k}\right)\frac{\partial k}{\partial x_j}\right] + P_k - \varepsilon \qquad (5)$$

$$U_j \frac{\partial \varepsilon}{\partial x_j} = \frac{\partial}{\partial x_j}\left[\left(\nu + \frac{\nu_t}{\sigma_\varepsilon}\right)\frac{\partial \varepsilon}{\partial x_j}\right] + C_1 P_k - \frac{\varepsilon}{k} - C_2\frac{\varepsilon^2}{k} \qquad (6)$$

$$P_k = \nu_t \frac{\partial U_i}{\partial x_j}\left(\frac{\partial U_i}{\partial x_j} + \frac{\partial U_j}{\partial x_i}\right) \qquad (7)$$

The model constants take the standard values for wind-tunnel flows:

$c_\mu = 0.09$, $c_1 = 1.44$, $c_2 = 1.92$, $\sigma_\kappa = 1.0$ and $\sigma_\varepsilon = 1.3$

To simulate a general airflow pattern, a high-rise building, shown in figure 2a, is considered. For comparison, the geometrical sizes of the building are 145m high, 31m wide and 31m deep in accordance with literature, in which, a corresponding scaled model (1:400) was measured in a wind tunnel test carried out by Stathopoulos, et al. The refuge floor, with height of 2.5m, is assigned in the middle of the building. The refuge floor is assigned as two types, i.e., open-floor (free of obstruction) and obstructed-floor (with a solid central core in the middle of refuge floor, fig 2b). Considering the symmetry of flow pattern, only half of the physical domain along the symmetrical plane is taken into account to save the computational cost (fig. 1a). A mesh scheme of $23 \times 6 \times 11$ grid nodes (length, height, width) is applied to refuge floor (fig. 1b). The whole flow domain is divided into $119 \times 79 \times 24$ control cells, see fig. 1b. A CFD simulation is carried out to predict airflow pattern around building and inside refuge floor by combining two meshes into one simulation. The inlet velocity conditions employ the power-law profile listed below:

$$\frac{u}{u_g} = \left(\frac{Z}{Z_g}\right)^\alpha, \; v = 0, \; w = 0 \qquad (8)$$

Where α is the open country exposure coefficient at the value of 0.15. Z_g is the gradient height, and u_g is the velocity at the height Z_g [Stathopolous, et al, 1989].

Previous studies show that the inlet conditions specified for turbulence greatly influence the flow around bluff body placed in atmospheric boundary layer [Stathopolous, et al, 1989]. For convenience, the turbulence intensity $I_u = \sqrt{u'^2}/U_0$ is established in accordance with the experimental conditions performed by Stathopoulos. The turbulence energy and its dissipation rate are approximated using following equations:

$$k(z) = 1.2 \cdot (I_u(z) \cdot U(z))^2, \quad \varepsilon(z) = \frac{C_\mu^{3/4} k(z)^{3/2}}{\kappa \cdot z} \tag{9}$$

All solid boundary conditions such as ground and building walls are evaluated by the well-known wall function [Launder, et al, 1974], in which the normal velocity is set to zero, the tangential velocity follows the logarithmic law $U(z) = U_\tau \ln(z/z_0)/\kappa$. All computations are proceeded by using CFD code based on finite-volume method, in which the above mathematical model has been installed.

III. Numerical Analysis and Discussion

The numerical results can be obtained by iterating the above discretized equations. The normalization of predicted pressure is based on the following formation:

Mean pressure coefficient: $C_p = \dfrac{p - p_0}{\frac{1}{2}\rho U_B^2}$ (U_B — front edge velocity on roof) (10)

Figure 3 shows the comparisons of predicted and measured [Stathopolous, et al, 1989] pressure coefficient on the windward side and the roof of the building. A good agreement between the measured and the predicted C_p values on the windward side can be observed. The largest deviation less than 5% can be found at the maximum pressure point, i.e., the front stagnation point of the building. The discrepancies between the measured and predicted pressure coefficients along the roof are countable. The reasons causing such deviations may be incurred by less sufficient meshes, the limitation of turbulence model currently used, etc. According to previous studies [Hunt, et al, 1978, Paterson, et al, 1990, Murakami, 1998, Ferziger, 1990], the separation region on roof for high-rise building is much larger than that for low-rise building and the drawback of k-ε model in predicting the reverse flow pattern over that part is revealed and, in the mean time, affects the accuracy of simulation. Advanced turbulence model will be needed to improve the quality of prediction. In addition to the effect of turbulence model, discrepancy may also be caused by other reasons such as the proper description of inlet boundary conditions, and the uncertainty of wind tunnel experiment [Stathopolous, et al, 1989].

According to Code of Practice on Means of Escape, a designated refuge floor should be open-sided on, at least, two sides to provide adequate cross ventilation. A very limited literature can be traced in this area. In this pioneer study, the building is assigned to three conditions, i.e., (i) with a designated refuge floor and free of obstruction; (ii) with a designated refuge floor and a central solid block; (iii) without refuge floor, see figure 2b. Same inlet boundary conditions are specified for all three cases. Figure 4a compares the pressure distributions on windward surface of the building with three conditions. The evident differences on three pressure curves can be noticed around the refuge floor. A sudden pressure variation exists due to the opening of refuge floor on the front edge of the building for both refuge floors. The pressures on windward surface are recovered to the same level as the case without refuge floor in a short distance after passing the opening of refuge floor. Figure 4b presents the pressure distributions on leeward surface of the building for all conditions. Under open-floor

condition, the pressure coefficient first reduces gradually, at the vicinity of refuge floor, decreases sharply to the lowest point within a very short distance. This is mainly caused by vorticity changes in separation region due to the flow crossing the refuge floor. The maximum reducing range in reverse pressure gradient is over 50% comparing to the highest point. It means that a strong flow separation region occurs behind the refuge floor for open-floor planning. The pressure gradually recovers, after the lowest point, to the normal level. The results of obstructed-floor show small differences from the case without refuge floor. Similar situations can be found on the roof surface in figure 4c. There are almost no differences on pressure distributions along the roof between the cases with obstructed-floor and the case without refuge floor. Whilst the pressure in open-floor is in the average higher than in the other two cases. From figure 4, the open-floor planning produces lower pressure at the inlet of refuge floor than the obstructed-floor does. The higher resistance from blocked refuge floor obstructs the flow through the refuge floor partly, and causes a high reverse pressure gradient. Comparisons of longitudinal velocity profiles between buildings with and without refuge floor along the main flow direction are shown in figure 5. From figure 5, little differences in velocity distributions can been observed between the situations with and without refuge floor except the area close to refuge floor. The location x/B=0.5 represents the centerline of the building. The zero velocity point on the downstream ground surface is identified as reattachment point. Corresponding to that point, the location x/B=6 is close to the reattachment region. The value of x/H is approximately 2.5, i.e., the reattachment length. It agrees with the wind tunnel test results [Stathopolous, et al, 1989], and also indicates that standard k-ε model is suitable for studying airflow fields in cases specified in the paper.

From the above analyses, it can be seen that geometrical configurations in refuge floor do affect the velocity distributions and further the smoke diffusion in refuge floor. The results imply that high speeds will be produced in open refuge floor, and may spread smoke quicker than that with obstructed planning once the smoke entering the refuge floor (fig. 4). The smoke is expected to be extracted or diluted as quickly as possible but, under obstructed-floor planning, may be trapped and circulated inside the floor due to the obstruction of central core, which is a typical design in high-rise buildings but not favorable to refuge floor. The study presented here can provide useful information to building designers on considering the planing of refuge floors within high-rise buildings.

IV. Conclusions

A detailed numerical analysis of airflow around and within the designated refuge floor of a high-rise building has been presented in the paper. Following conclusions can be drawn:

1. Generally, the numerical results of wind loading on building surfaces express good and satisfactory agreements with the corresponding experimental data;
2. The presence of designated refuge floor have little influence on the airflow field around the building, so the total building responses to external environmental impact will not be affected;
3. The airflow pattern within the refuge floor is greatly influenced by the geometrical characteristics of the floor, and will further affect the smoke diffusion inside the refuge floor;
4. The refuge floor with open planning may assist to extract the smoke once it entering the floor, while the obstructed refuge floor case may retards the smoke expelling due to the geometrical blockage;
5. Further studies are required to help understand the smoke migration within the refuge floor and the effect of external airflow conditions on the smoke diffusions.

Acknowledgment

The authors acknowledge the support of Strategic Research Grant # 7000794, City University of Hong Kong.

References

Code of Practice on Means of Escape, Hong Kong, Hong Kong Government, 1996.
Egan, M D, *Concepts in building fire safety*, Robert Krieger Publishing Co., 1986.
Lo, S M (1998), The Use of Designated Refuge Floors in High-rise Buildings: Hong Kong Perspective, *Journal of Applied Fire Science*, 7:3, 287-299.
Hunt J R C, Abell C J & Peterka J A (1978), Kinematical studies of the around free or surface-mounted obstacles-applying topology to flow-visualization, *Journal of Fluid Mechanics*, 86, 179-200.
Paterson D A & Colin J A (1990), Simulation of flow past a cube in turbulent boundary layer, *Journal of Wind Engineering & Industrial Aerodynamics*, 35, 149-176.
Stathopoulos T & Brulotte M D, (1989), Design recommendations for wind loading on buildings of intermediate height, *Canadian Journal of Civil Engineering*, 16, 910-916D.
Murakami S, (1998) Overview of turbulence models applied in CWE-1997, *Journal of Wind Engineering & Industrial Aerodynamics*, 74-76, 1-24.
Ferziger J H, (1990) Approaches to turbulent flow computation: Application to flow over obstacles, *Journal of Wind Engineering & Industrial Aerodynamics*, 35, 1-19.
Launder B E & Spalding D B, (1974), The numerical computation of turbulent flows, *Computer Methods in Applied Mechanics and Engineering*, 3, 269-289.

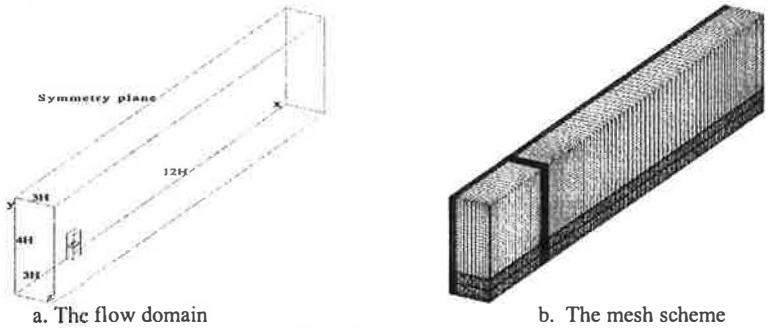

a. The flow domain b. The mesh scheme

Figure 1 The geometrical configuration and mesh scheme (H — Building height)

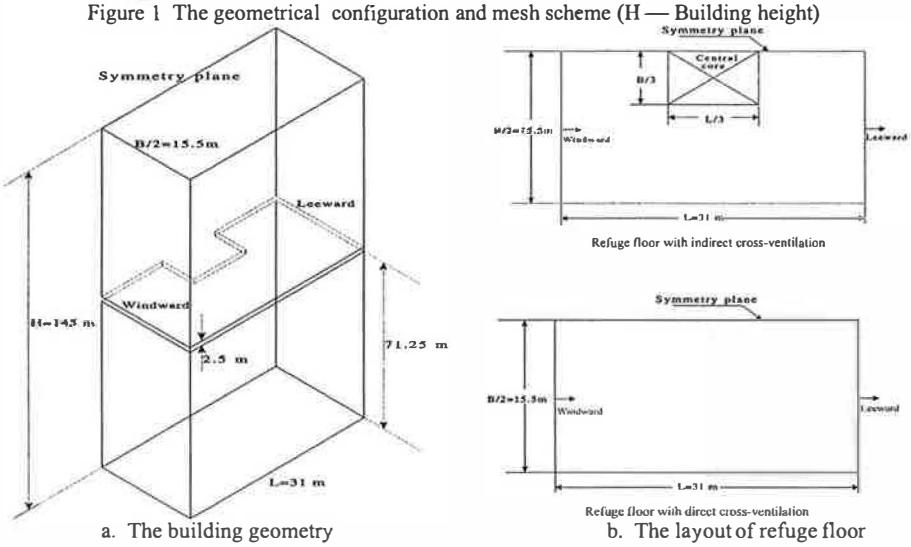

a. The building geometry b. The layout of refuge floor

Figure 2 The outlines of model building

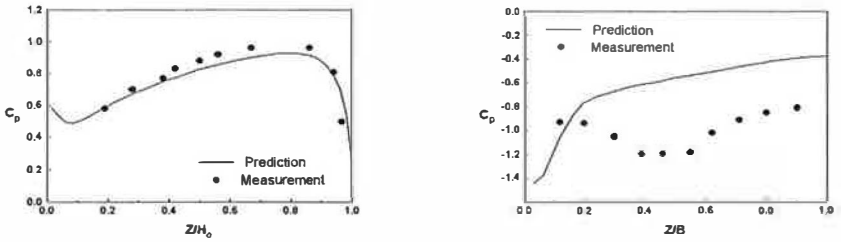

a. Pressure distribution on winward surface b. Pressure distribution on roof

Figure 3 Comparison of pressure coefficients between predictions and measurements

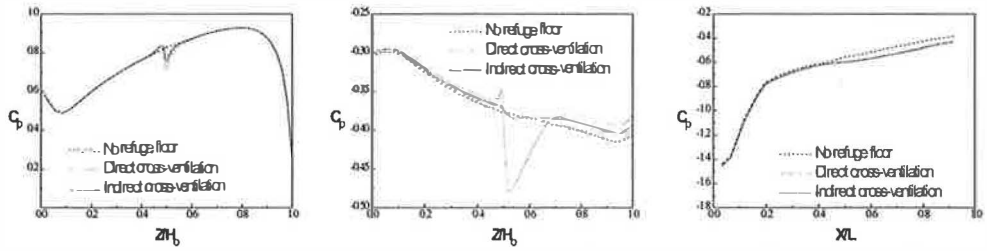

a. Pressure on winward side b. Pressure on leeward side c. Pressure on roof

Figure 4 Pressure distributions on building surfaces

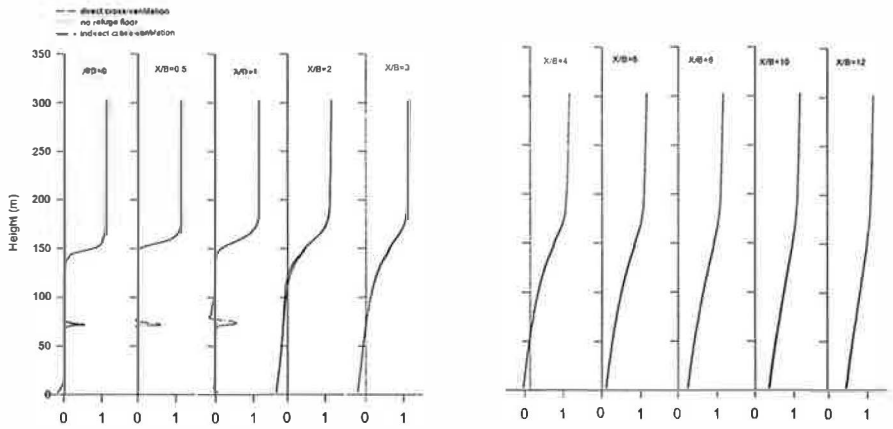

Figure 5 Longitudinal velocities in the symmetry plane of the building along the main flow direction